Supporting Information

Broad-band Emission in a Zero-Dimensional Hybrid Organic [$PbBr_6$] Trimer with Intrinsic Vacancies

Jun Zhou[#,†], Mingze Li[#,†], Lixin Ning[*,‡], Ruiling Zhang[§], Maxim S. Molokeev[⊥,△,◊], Jing Zhao[†], Songqiu Yang[§], Keli Han[§], and Zhiguo Xia[*,†,♀]

[†] The Beijing Municipal Key Laboratory of New Energy Materials and Technologies, School of Materials Sciences and Engineering, University of Science and Technology Beijing, Beijing, 100083, China

[‡] Anhui Key Laboratory of Optoelectric Materials Science and Technology, Key Laboratory of Functional Molecular Solids, Ministry of Education, Anhui Normal University, Wuhu, Anhui, 241000, China

[§] Dalian Institute of Chemical Physics, Chinese Academy of Sciences, Dalian, 116000, China

[⊥] Laboratory of Crystal Physics, Kirensky Institute of Physics, Federal Research Center KSC SB RAS, Krasnoyarsk 660036, Russia

[△] Siberian Federal University, Krasnoyarsk, 660041, Russia

[◊] Department of Physics, Far Eastern State Transport University, Khabarovsk, 680021, Russia

[♀] State Key Laboratory of Luminescent Materials and Devices and Institute of Optical Communication Materials, South China University of Technology, Guangzhou, 510641, China

Corresponding Author

[*]xiazg@ustb.edu.cn

[*]ninglx@mail.ahnu.edu.cn

EXPERIMENTAL DETAILS

Materials and Preparation. All the chemicals were commercially purchased and used without further purification. 1-buty-1-methylpyrrolidinium bromide ($C_9NH_{20}Br$) and lead bromide ($PbBr_2$) were dissolved in dimethylformamide (DMF) in the molar ratio of 4:1, 5:1, 6:1 and 7:1. Then filtered to achieve a clear precursor solution. After addition of acetone, the solution was left undisturbed for 36 h to yield dark yellow crystals of $(C_9NH_{20})_6Pb_3Br_{12}$. This solid was filtered out and then washed with acetone and finally dried under reduced pressure overnight. All the samples are pure phase. Hence, without special instructions, the following tests are all characterized by 4:1 samples.

Characterization. Single crystal X-ray diffraction data of $(C_9NH_{20})_6Pb_3Br_{12}$ was collected at 293 K using the XtaLAB AFC12 (RINC) four-circle X-ray single crystal diffractometers (Rigaku) equipped with a CCD-detector, rotating-anode Mo Kα tube and graphite monochromator. The absorption corrections and frames scaling were applied using the empirical correction (ABSPACK) program. The structures were solved by the direct methods using package SHELXS and refined in the anisotropic approach for non-hydrogen atoms using the SHELXL program.[1] All hydrogen atoms were found via Fourier difference maps. Further the hydrogen atoms which are linked with C atoms were positioned geometrically as riding on their parent atoms with d(C–H) = 0.93-0.98 Å depending on geometry and Uiso(H) = 1.2Ueq(C,N). The structure test for the presence of missing symmetry elements and possible voids was produced using the program PLATON.[2] The DIAMOND program is used for the crystal structure plotting.[3] Powder X-ray diffraction data of $(C_9NH_{20})_6Pb_3Br_{12}$ was obtained using diffractometer D8 ADVANCE (Bruker) equipped by a VANTEC detector with a Ni filter. The measurements were made using Cu Kα radiation. The structural parameters defined by single crystal analysis were used as a basic in powder pattern Rietveld refinement. The refinement was produced using TOPAS 4.2 software.[4] The optical microscope photographs of crystal sample were obtained by using a Nikon LV100ND optical microscope. The morphology and particle size of the powder sample was characterized by scanning electron microscope (SEM, JEOL JSM-6510) and the inorganic elemental composition was determined using energy dispersive X-ray spectroscopy (EDS) that was attached to the SEM. Elemental analysis (C, H and N) of the samples was performed in a vario MACRO cube (Elementar Analysensysteme Gmbh, Germany). The absorption spectra were measured on a UV-Vis-NIR spectrophotometer (SHIMADZU UV-3600) supplied with an integrating sphere. The room temperature excitation (PLE), room temperature emission spectra (PL), the room-temperature decay curves, and photoluminescence quantum efficiency (PLQE) were obtained using a FLSP9200 fluorescence spectrophotometer (Edinburgh Instruments Ltd., U.K.). Thermogravimetric analysis (TGA) were performed on a Setaram Labsys Evo at 10 ^{o}C min^{-1} in an argon flow from room temperature to 800 ^{o}C. TA experiments were performed by using a home-made femtosecond pump-probe setup.[5] Laser pulses (800 nm, 50 fs pulse length, 1 kHz repetition rate) were generated by a Ti:sapphire

femtosecond laser (Hurricane, Spectra-Physics) source. An optical parametric amplifier was used to change the laser wavelength. For the probe we used the super-continuum generation from a thin CaF plate. The sample was excited by 320 nm laser pulse. The X-ray photoelectron spectroscopy (XPS) spectra were obtained using an XPS spectrometer (ESCSLAB 250Xi).

Computational methodology. The unit cell of $(C_9NH_{20})_6Pb_3Br_{12}$ containing 585 atoms was employed for periodic DFT investigations using the VASP code.[6-7] The $C(2s^22p^2)$, $N(2s^22p^3)$, $H(1s^1)$, $Pb(6s^26p^2)$, and $Br(4s^24p^5)$ were treated as valence electrons, and their interactions with the cores were described by the projected augmented wave (PAW) approach.[8] The atomic positions in the unit cell were optimized with the pure PBE functional,[9] with the lattice parameters fixed at the experimental values. The thermodynamic charge transition levels of crystal defects were calculated with the PBE0 hybrid functional,[10] on the basis of the PBE-optimized atomic structure. One k-point Γ was used to sample the Brillouin zone, and the cutoff energy of the plane-wave basis was set to 400 eV. Due to the strong spin-orbit coupling effect on Pb, this effect was included throughout the calculations.

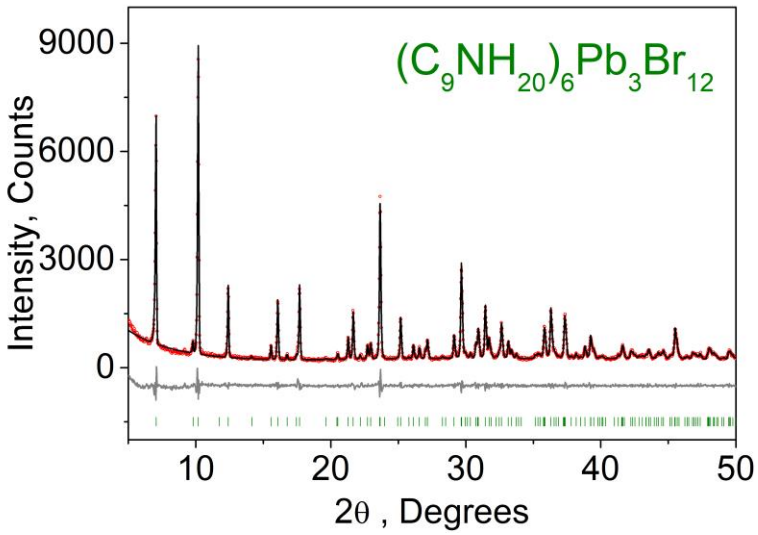

Figure S1. Difference X-ray powder pattern of $(C_9NH_{20})_6Pb_3Br_{12}$.

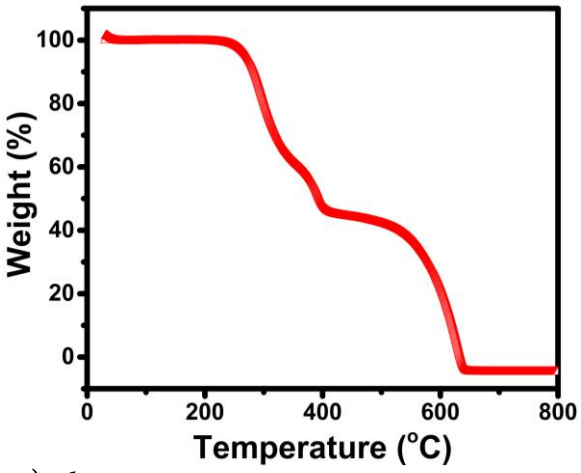

Figure S2. TGA data of $(C_9NH_{20})_6Pb_3Br_{12}$ crystals.

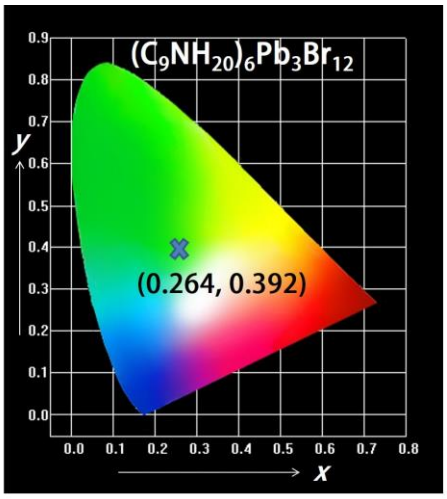

Figure S3. CIE chromaticity diagram of $(C_9NH_{20})_6Pb_3Br_{12}$ crystals.

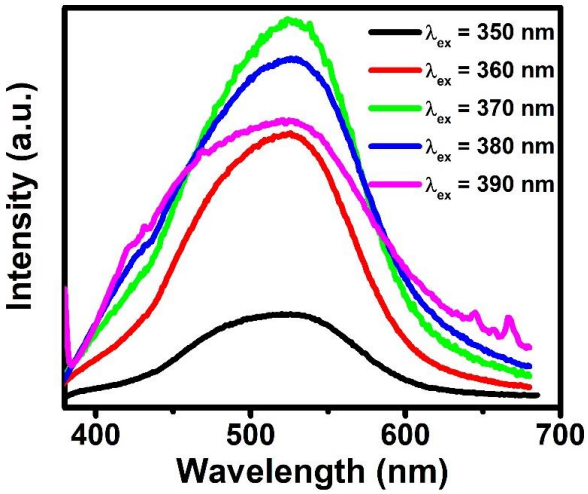

Figure S4. The excitation-wavelength-dependent PL spectra of $(C_9NH_{20})_6Pb_3Br_{12}$ at room temperature.

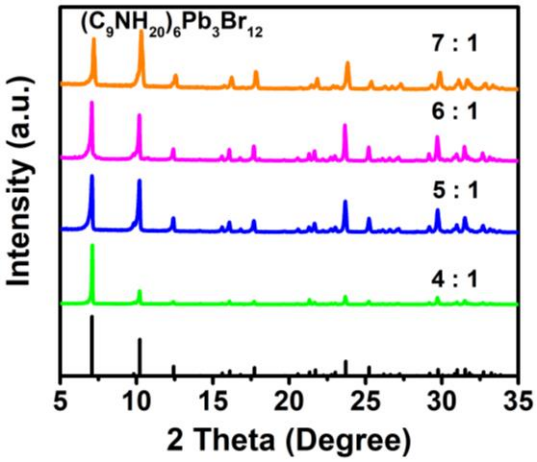

Figure S5. XRPD patterns of $(C_9NH_{20})_6Pb_3Br_{12}$ with different molar ratio of $C_9NH_{20}Br$ and $PbBr_2$ of 4:1, 5:1, 6:1 and 7:1.

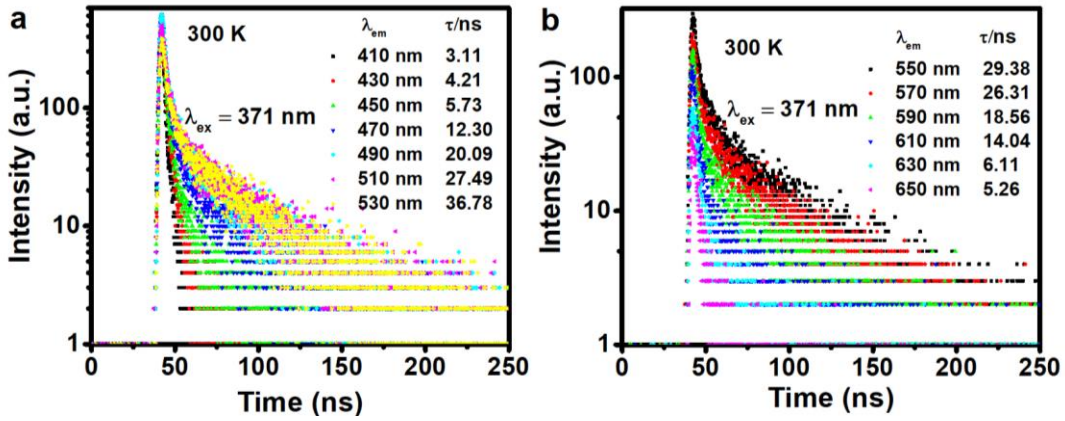

Figure S6. (a) and (b) The nanosecond photoluminescence decay of $(C_9NH_{20})_6Pb_3Br_{12}$ bulk crystals for different emission wavelength in the broad emission (410 nm – 650 nm) excited by 371 nm at room temperature.

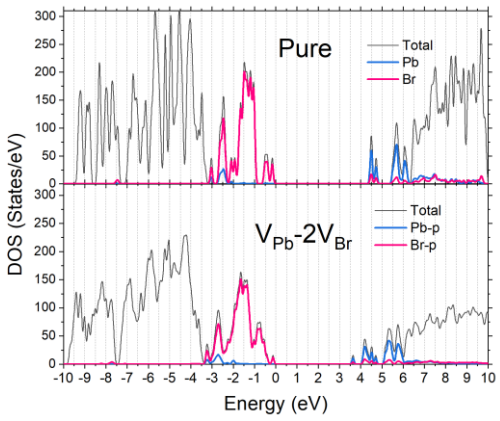

Figure S7. A comparison of total and orbital-projected DOS for the pure and the most stable V_{Pb}–$2V_{Br}$-incorporated $(C_9NH_{20})_6Pb_3Br_{12}$ obtained with the DFT-PBE0 method.

Table S1. Main parameters of processing and Rietveld refinement of the $(C_9NH_{20})_6Pb_3Br_{12}$.

Compound	$(C_9NH_{20})_6Pb_3Br_{12}$
Sp.Gr.	*R*-3
a, Å	17.3606 (7)
c, Å	22.579 (1)
V, Å^3	5893.4 (6)
Z	9
2ϑ-interval, º	5-50
R_{wp}, %	7.74
R_p, %	5.86
R_{exp}, %	4.36
χ^2	1.78

Table S2. Crystal structure parameters of $(C_9NH_{20})_6Pb_3Br_{12}$.

Single crystal	$(C_9NH_{20})_6Pb_3Br_{12}$
Moiety formula	$C_{18}H_{40}Br_4N_2Pb$
Dimension (mm)	0.02×0.01×0.005
Color	Colorless
Molecular weight	811.35
Temperature (K)	293 (2)
Space group, *Z*	*R*-3, 9
a (Å)	17.3128 (8)
c (Å)	22.5186 (11)
V (Å^3)	5845.3 (6)
ρ_{calc} (g/cm^3)	2.074
μ (mm^{-1})	12.652
Reflections measured	13835
Reflections independent	3341
Reflections with $F > 4\sigma(F)$	2635

$2\theta_{max}$ (°)	60.812
h, *k*, *l* - limits	-22 ≤ *h* ≤ 23; -24 ≤ *k* ≤ 23; -30 ≤ *l* ≤ 31
R_{int}	0.0285
The weighed refinement of F^2	$w=1/[\sigma^2(F_o^2)+(0.0373P)^2+6.0635P]$
Number of refinement parameters	117
$R1$ [$F_o > 4\sigma(F_o)$]	0.0258
*wR*2	0.0653
Goof	1.033
$\Delta\rho_{max}$ (e/Å^3)	0.808
$\Delta\rho_{min}$ (e/Å^3)	-0.733
$(\Delta/\sigma)_{max}$	0.002

Table S3. Fractional atomic coordinates and isotropic or equivalent isotropic displacement parameters (Å^2).

	x	*y*	*z*	U_{iso}*/U_{eq}
Pb1	2/3	1/3	1/3	0.04665 (9)
Pb2	2/3	1/3	0.51498 (2)	0.04738 (8)
Br1	0.70285 (3)	0.48589 (3)	0.41611 (2)	0.06140 (12)
Br2	0.81078 (3)	0.47991 (3)	0.58042 (2)	0.07637 (14)
C1	0.3407 (4)	0.4098 (4)	0.4446 (3)	0.0965 (17)
H1A	0.3775	0.4683	0.4621	0.116*
H1B	0.2850	0.4048	0.4315	0.116*
C2	0.3237 (5)	0.3391 (4)	0.4882 (3)	0.111 (2)
H2A	0.2665	0.3179	0.5075	0.133*
H2B	0.3700	0.3611	0.5182	0.133*
C3	0.3240 (5)	0.2645 (4)	0.4517 (3)	0.117 (2)
H3A	0.2665	0.2103	0.4545	0.140*

H3B	0.3694	0.2522	0.4664	0.140*
C4	0.3438 (4)	0.2972 (4)	0.3867 (3)	0.105 (2)
H4A	0.3830	0.2796	0.3679	0.126*
H4B	0.2893	0.2742	0.3638	0.126*
N5	0.3884 (3)	0.3961 (3)	0.39331 (19)	0.0781 (11)
C6	0.3930 (4)	0.4481 (4)	0.3385 (3)	0.0948 (16)
H6A	0.4242	0.5110	0.3487	0.114*
H6B	0.4288	0.4392	0.3091	0.114*
C7	0.3083 (5)	0.4265 (5)	0.3112 (3)	0.113 (2)
H7A	0.2669	0.4232	0.3416	0.135*
H7B	0.2827	0.3688	0.2919	0.135*
C8	0.3226 (6)	0.4981 (8)	0.2654 (4)	0.154 (3)
H8A	0.3512	0.5559	0.2848	0.185*
H8B	0.3627	0.4996	0.2348	0.185*
C9	0.2470 (9)	0.4847 (12)	0.2398 (5)	0.269 (8)
H9A	0.1983	0.4283	0.2524	0.322*
H9B	0.2530	0.4849	0.1974	0.322*
H9C	0.2356	0.5315	0.2513	0.322*
C10	0.4825 (4)	0.4301 (4)	0.4098 (3)	0.1014 (18)
H10A	0.4853	0.4103	0.4491	0.122*
H10B	0.5141	0.4941	0.4088	0.122*
H10C	0.5092	0.4081	0.3822	0.122*

Table S4. Main geometric parameters (Å, º) of $(C_9NH_{20})_6Pb3Br_{12}$.

Pb1—Br1^{i}	3.0312 (4)	C4—H4A	0.9700
Pb1—Br1	3.0312 (4)	C4—H4B	0.9700
Pb1—Br1^{ii}	3.0312 (4)	N5—C10	1.476 (7)

Pb1—Br1^{iii}	3.0312 (4)	N5—C6	1.506 (7)
Pb1—Br1^{iv}	3.0313 (4)	C6—C7	1.456 (9)
Pb1—Br1^{v}	3.0313 (4)	C6—H6A	0.9700
Pb2—Br2^{ii}	2.9164 (5)	C6—H6B	0.9700
Pb2—Br2^{iii}	2.9164 (5)	C7—C8	1.535 (11)
Pb2—Br2	2.9164 (5)	C7—H7A	0.9700
C1—C2	1.478 (8)	C7—H7B	0.9700
C1—N5	1.507 (6)	C8—C9	1.340 (13)
C1—H1A	0.9700	C8—H8A	0.9700
C1—H1B	0.9700	C8—H8B	0.9700
C2—C3	1.533 (8)	C9—H9A	0.9600
C2—H2A	0.9700	C9—H9B	0.9600
C2—H2B	0.9700	C9—H9C	0.9600
C3—C4	1.544 (9)	C10—H10A	0.9600
C3—H3A	0.9700	C10—H10B	0.9600
C3—H3B	0.9700	C10—H10C	0.9600
C4—N5	1.492 (6)		
Br1^{i}—Pb1—Br1	93.854 (12)	Br1^{iii}—Pb1—Br1^{iv}	180.0
Br1^{i}—Pb1—Br1^{ii}	180.0	Br1^{i}—Pb1—Br1^{v}	86.147 (12)
Br1—Pb1—Br1^{ii}	86.148 (12)	Br1—Pb1—Br1^{v}	180.0
Br1^{i}—Pb1—Br1^{iii}	93.853 (12)	Br1^{ii}—Pb1—Br1^{v}	93.851 (12)
Br1—Pb1—Br1^{iii}	86.149 (12)	Br1^{iii}—Pb1—Br1^{v}	93.853 (12)
Br1^{ii}—Pb1—Br1^{iii}	86.148 (12)	Br1^{iv}—Pb1—Br1^{v}	86.146 (12)
Br1^{i}—Pb1—Br1^{iv}	86.148 (12)	Br2^{ii}—Pb2—Br2^{iii}	96.719 (15)
Br1—Pb1—Br1^{iv}	93.853 (12)	Br2^{ii}—Pb2—Br2	96.718 (15)
Br1^{ii}—Pb1—Br1^{iv}	93.851 (12)	Br2^{iii}—Pb2—Br2	96.718 (15)

Symmetry codes: (i) *x*-*y*+1/3, *x*-1/3, -*z*+2/3; (ii) -*x*+*y*+1, -*x*+1, *z*; (iii) -*y*+1, *x*-*y*, *z*; (iv) *y*+1/3, -*x*+*y*+2/3, -*z*+2/3; (v) -*x*+4/3, -*y*+2/3, -*z*+2/3.

Table S5. Hydrogen-bond geometry in $(C_9NH_{20})_6Pb_3Br_{12}$ structure (Å, °).

D—H	d(D—H)	d(H···A)	∠ D—H···A	D···A	A	Transformation for A atom
C6—H6A	0.97	2.89	158	3.806 (6)	Br2	y, 1-x+y, 1-z

Table S6. EA analysis of $(C_9NH_{20})_6Pb_3Br_{12}$ samples.

compound	mass %			mole ratio C:H:N
	C (%)	H (%)	N (%)	
theoretical	26.64	4.93	3.45	9: 20: 1
sample 1	26.46	4.25	3.62	8.5: 16.4: 1
sample 2	25.67	4.28	3.41	8.8: 17.6: 1

References

(1) Sheldrick, G. M. A Short History of SHELX. *Acta Cryst.* **2008,** *64,* 112-122.
(2) PLATON – A Multipurpose Crystallographic Tool. Utrecht University, Utrecht. The Netherlands, **2008**.
(3) Brandenburg, K.; Berndt, M. Diamond: Visual Crystal Structure Information System CRUSTAL IMPACT. *Postfach.* **2004**.
(4) Topas, V. General Profile and Structure Analysis Software for Powder Diffraction Data-User's Manual. Bruker AXS: Karlsruhe, Germany. **2008**.
(5) Yang, B.; Chen, J. S; Yang, S. Q; Hong, F.; Sun, L.; Han, P. G; Pullerits, T.; Deng, W. Q; Han, K. L. Lead-Free Silver-Bismuth Halide Double Perovskite Nanocrystals. *Angew. Chem.* **2018,** *57,* 5359-5363.
(6) Kresse, G.; Furthmüller, Efficient Iterative Schemes for ab initio Total-Energy Calculations Using a Plane-wave basis Set. *J. Phys. Rev. B: Condens. Matter Mater. Phys.* **1996,** *54,* 11169–11186.
(7) Kresse, G.; Joubert, D. From Ultrasoft Pseudopotentials to the Projector Augmented-Wave Method. *Phys. Rev. B: Condens. Matter Mater. Phys.* **1999,** *59,* 1758–1775.
(8) Blöchl, P. E.. Projector Augmented-Wave Method. *Phys. Rev. B.* **1994,** *50,* 17953-17979.
(9) Perdew, J. P.; Burke, K.; Ernzerhof, M. Generalized Gradient Approximation Made Simple. *Phys. Rev. Lett.* **1996,** *77,* 3865–3868.
(10) Perdew, J. P.; Ernzerhof, M.; Burke, K. Rationale for Mixing Exact Exchange with Density Functional Approximations. *J. Chem. Phys.* **1996,** *105,* 9982-9985.